Estimation of Tire Load and Vehicle Parameters Using Intelligent Tires Combined with Vehicle Dynamics

Dasol Jeong, Seungtaek Kim, Jonghyup Lee, Seibum B. Choi, *Member, IEEE,* Mintae Kim and Hojong Lee

***Abstract*—This paper focuses on estimation of static/dynamic tire load and vehicle parameters using intelligent tires and vehicle dynamics. This study is conducted to improve and ensure the performance of advanced vehicle control using accurate vehicle and tire states. Contact angle between tire and road surface is calculated by intelligent tire and is used for tire load estimation. The tire load estimation results are validated by flexible ring tire model. For fast sampling rate and high robustness, a new estimation algorithm, which combines intelligent tire and vehicle dynamics, is proposed in this paper. Not only the tire load but also the vehicle parameters such as total mass, center of gravity point(CG point) and center of gravity height(CG height) are estimated by the proposed estimation algorithm. The proposed estimation algorithm is verified by indoor test using Flac trac(tire test system) and real-time test using AutoBox III. In short, the estimation algorithm proposed in this paper can estimate static/dynamic tire load and vehicle parameters with fast sampling rate and high robustness.**

***Index Terms*—Tire load, Vehicle parameter, Intelligent tires, Flexible ring tire model, Load transfer, Multi Input Multi Output(MIMO) system**

I. Introduction

TIRES contain lots of information because they are the only part of the vehicle that come into contact with the road surface. Tires play many roles in acceleration, deceleration, and steering situations of vehicle movement where force and moment occur between the tire and the road surface. Therefore, estimating the information contained in the tire is becoming a very important study in vehicle control. Informations contained in the tire, such as load applied to each wheel of the vehicle, play a very important role, in particular, for vehicle control and various vehicle parameter estimation. Total load of the vehicle and the load applied to each tire are directly related to the performance and accuracy of model-based control [1], [2], power-train system [3], ABS system(Anti-lock braking system) [4] and road slope estimation [5].

Total vehicle load, CG point(center of gravity point) and CG height(center of gravity height) of the vehicle are parameters that can be changed up to 30% depending on the weight of the passengers or cargoes [6]. However, many vehicle dynamics-related fields and chassis control systems assume that these parameters are known and proceed the algorithm development. As a result, the performance of those algorithms is not fully utilized. For example, wrong information of the vehicle load directly affects braking distance prediction, shift timing control, or battery management in hybrid vehicles. Due to the importance of vehicle load information, many studies have been conducted to estimate vehicle load. Previous studies have proposed vehicle load estimation algorithms using Kalman filters [7], recursive least squares [8], [9], nonlinear filters [10], hybrid shock absorber model [11], adaptive observer [12] and payload parameter estimator [13] based on vehicle sensors and vehicle dynamics. However, these previous algorithms are slow and show about 10% error, depending on the road slope and air resistance.

Estimation of vehicle mass and CG point is an important research topic not only in the field of vehicle dynamics, but also in the field of measurement and instrumentation. Because there is no commercialized system that directly measures vehicle load and CG point in real-time. In previous studies, new sensors and systems have been developed to estimate the vehicle mass and CG point. A low-cost on-board vehicle load monitor system for the heavy vehicle [14], a vision-based non-contact vehicle weigh-in-motion method [15], and a high precision gravity center measure system in offline [16] have been proposed. In addition, a measurement algorithm for CG points of various plants has been proposed [17]. In this way, new sensors and algorithms are being studied to estimate mass and CG points in the field of measurement and measurement. In this study, we intend to contribute to the field of measurement and measurement through the proposed vehicle mass and CG point estimation algorithm.

From the perspective of vehicle control, tire load information is as important as vehicle mass information. Such studies have proposed tire load estimation algorithms based on the longitudinal/lateral acceleration sensors in the vehicle [10]. There are several limitations in previous studies of tire load estimation. First, total vehicle load and position of center of gravity are incorrect. Total load and position of center of gravity are parameters that vary up to 30% depending on the vehicle condition. Therefore, errors due to incorrect total vehicle load and position of center of gravity can cause a large error in estimating tire load. Also, previous study algorithms can only be applied to accelerating, decelerating or steering driving condition. Therefore, in this paper, a new load estimation strategy is introduced that combines vehicle dynamics and intelligent tires.

Intelligent tires are new concept tires with an additional

Dasol Jeong, Seungtaek Kim, Jonghyup Lee and Seibum B. Choi are with the Korea Advanced Institute of Science and Technology, Daejeon 34141, South Korea (e-mail: oieiaa@kaist.ac.kr; kimst9o9@kaist.ac.kr; sonic_92@kaist.ac.kr; sbchoi@kaist.ac.kr)

Mintae Kim and Hojong Lee are with the HANKOOK TIRE CO. LTD, Daejeon 34127, South Korea (e-mail: mtkim@hankooktire.com, lhojong@vt.edu).

sensor installed inside the tire [18]. Intelligent tires are designed to estimate important but difficult-to-find information of tires. Recently, researches on such intelligent tires have been actively conducted such as estimation of tire wear [19], [20], tire load [21], [22], [23] road surface [24], [25], vehicle state such as side slip [26], [27], contact property [28], [29], tire deformation [30] and longitudinal force [31]. However, most intelligent tire research were based on data-based phenomena observation. These methods have a limitation of not guaranteeing the generality and robustness of the estimation method.

In this paper, tire load estimation algorithm using intelligent tire is proposed. For validation of the estimation method, flexible ring tire model, a physical model of the tire, is used for verification for estimation generality and robustness. The flexible ring tire model is a tire model which describes the deformation of the tire especially for the position where the tire sensor is attached in the intelligent tire [27], [32]. Intelligent tire based tire load estimation has good performance. However, there are following limitations. First, the sampling rate is very slow, which is one estimation of tire load per tire revolution [33]. Second, it has low robustness. Static tire load of each wheel is impossible to be estimated at general driving situations where acceleration, deceleration and steering exist [21]. To overcome this, a new tire load compensation algorithm is proposed in this paper which combines vehicle dynamics with intelligent tire. In conclusion, the proposed estimation algorithm has three advantages. First, it has high sampling rate. Second, it has high robustness at estimating static/dynamic tire load for general driving. Third, vehicle parameters such as CG point and CG height can be estimated.

Indoor tests were conducted to verity load estimation algorithm using intelligent tires through the Flat trac experiment as shown in Fig. 1. For indoor experiments, data were obtained for 2 seconds under 96 conditions as shown in Table. I. The sampling rate of the acceleration sensor inside the intelligent tire is 9600 Hz. These data were used to develop intelligent tire based tire load estimation method and verify the estimation method. Real-vehicle experiments were conducted to verify the performance of the new estimation algorithm which combines intelligent tire based tire load estimation and vehicle dynamics. Intelligent tire sensor signal of each tire, wheel velocity signal, and IMU sensor signal were received, and the tire load and vehicle parameters were estimated and analyzed in real time using Autobox 3.0 with real time interface.

TABLE I
TIRE CONDITIONS OF INDOOR EXPERIMENTS

Tire condition	Value
Tire load	40% 100% 160% (100% =5000N)
Velocity	30km/h, 65km/h
Pressure	1.3bar, 1.7bar, 2.1bar, 2.4bar
Tire wear	0mm, 2mm, 4mm, 6mm (0mm: new tire)

The rest of the paper is organized as follows. In section II, the linear load transfer model using vehicle dynamics is introduced. The tire load estimation algorithm using intelligent tire is proposed in section III. In section IV, an algorithm which combines intelligent tire and vehicle dynamics for estimating static/dynamic tire load and vehicle parameters is proposed. Experimental validation is presented in section V, and conclusions are provided in section VI.

Fig. 1. Flat trac

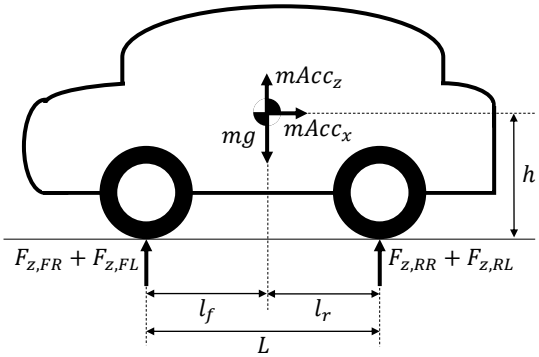

(a) Side view half-car model

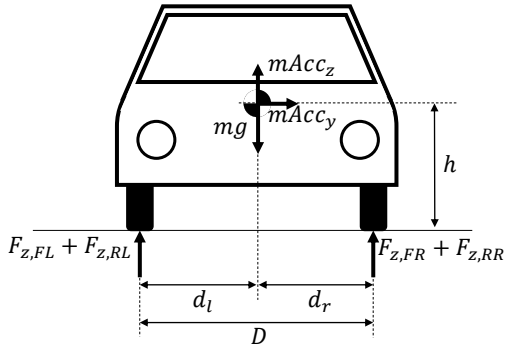

(b) Front view half-car model

Fig. 2. Vehicle dynamics model

II. VEHICLE DYNAMICS MODEL

A. Nonlinear Load Transfer Model

Fig. 2 shows the vehicle dynamics model used in this study [10]. It is assumed that the vehicle model is a rigid body. The model parameters are total mass (m), CG point (l_r, d_l), CG height (h), vehicle specifications (L, D) and pitch/roll moment of inertia(I_{yy}, I_{xx}). States are 3-axis acceleration(Acc_x, Acc_y, Acc_z), pitch/roll rate(ω_p, ω_r) and

TABLE II
LOAD TRANSFER MODEL PARAMETER

Symbol	Parameter	Unit
m	Front right tire load	kg
I_{yy}	Pitch moment of inertia	kgm^2
I_{xx}	Roll moment of inertia	kgm^2
l_f	Center of gravity longitudinal position	m
d_l	Center of gravity lateral position	m
h	Center of gravity height	m
$F_{z,FR}$	Front right tire load	N
$F_{z,FL}$	Front left tire load	N
$F_{z,RR}$	Rear right tire load	N
$F_{z,RL}$	Rear left tire load	N
Acc_x	Longitudinal acceleration of vehicle	m/s^2
Acc_y	Lateral acceleration of vehicle	m/s^2
Acc_z	Vertical acceleration of vehicle	m/s^2
$\dot{\omega}_p$	Pitch rate of vehicle	rad/s
$\dot{\omega}_r$	Roll rate of vehicle	rad/s

each tire load($F_{Z,FR}, F_{Z,FL}, F_{Z,RR}, F_{Z,RL}$). (1) represents the load of each tire through force/momentum equilibrium equation [10].

$$\begin{aligned}
F_{Z,FR} &= mg\left(\frac{l_r}{L} - \frac{h}{L}\frac{Acc_x}{g} - \frac{l_r}{L}\frac{Acc_z}{g} + \frac{I_{yy}}{mgL}\dot{\omega}_p\right) \\
&\quad \times \left(\frac{d_l}{D} + \frac{h}{D}\frac{Acc_y}{g} - \frac{d_l}{D}\frac{Acc_z}{g} - \frac{I_{xx}}{mgD}\dot{\omega}_r\right) \\
F_{Z,FL} &= mg\left(\frac{l_r}{L} - \frac{h}{L}\frac{Acc_x}{g} - \frac{l_r}{L}\frac{Acc_z}{g} + \frac{I_{yy}}{mgL}\dot{\omega}_p\right) \\
&\quad \times \left(\frac{d_r}{D} - \frac{h}{D}\frac{Acc_y}{g} - \frac{d_r}{D}\frac{Acc_z}{g} + \frac{I_{xx}}{mgD}\dot{\omega}_r\right) \\
F_{Z,RR} &= mg\left(\frac{l_f}{L} + \frac{h}{L}\frac{Acc_x}{g} - \frac{l_f}{L}\frac{Acc_z}{g} - \frac{I_{yy}}{mgL}\dot{\omega}_p\right) \\
&\quad \times \left(\frac{d_l}{D} + \frac{h}{D}\frac{Acc_y}{g} - \frac{d_l}{D}\frac{Acc_z}{g} - \frac{I_{xx}}{mgD}\dot{\omega}_r\right) \\
F_{Z,RL} &= mg\left(\frac{l_f}{L} + \frac{h}{L}\frac{Acc_x}{g} - \frac{l_f}{L}\frac{Acc_z}{g} - \frac{I_{yy}}{mgL}\dot{\omega}_p\right) \\
&\quad \times \left(\frac{d_r}{D} - \frac{h}{D}\frac{Acc_y}{g} - \frac{d_r}{D}\frac{Acc_z}{g} + \frac{I_{xx}}{mgD}\dot{\omega}_r\right)
\end{aligned} \tag{1}$$

(1) shows the load transfer of each wheel as a result of vehicle motion. Each tire load is expressed as the product of several accelerations/angular velocities. This means that the Load Transfer model is nonlinear. Nonlinear models are complex and negatively affect the computational speed, and robustness of the algorithm. Therefore, in this paper, we used a linear load transfer model through physical assumptions.

B. Linear Load Transfer Model

This section describes the linear load transfer model and the physical assumptions used. (1) shows the load of each wheel from the nonlinear load transfer model. For linearization of the load transfer model, tire load was analyzed by dividing by front/rear tire force ($F_{Z,FR}+F_{Z,FL}, F_{Z,RR}+F_{Z,RL}$) and left/right tire force ($F_{Z,FR}+F_{Z,RR}, F_{Z,FL}+F_{Z,RL}$) as shown in Figure 2. (2) represents the front/rear tire load right/left tire load respectively.

$$\begin{aligned}
F_{Z,FR} + F_{Z,FL} &= \frac{l_r}{L}mg - \frac{h}{L}mAcc_x - \frac{l_r}{L}mAcc_z + \frac{I_{yy}}{L}\dot{\omega}_p \\
F_{Z,RR} + F_{Z,RL} &= \frac{l_f}{L}mg + \frac{h}{L}mAcc_x - \frac{l_f}{L}mAcc_z - \frac{I_{yy}}{L}\dot{\omega}_p \\
F_{Z,FR} + F_{Z,RR} &= \frac{d_l}{D}mg + \frac{h}{D}mAcc_y - \frac{d_l}{D}mAcc_z - \frac{I_{xx}}{D}\dot{\omega}_r \\
F_{Z,FL} + F_{Z,RL} &= \frac{d_r}{D}mg - \frac{h}{D}mAcc_y - \frac{d_r}{D}mAcc_z + \frac{I_{xx}}{D}\dot{\omega}_r
\end{aligned} \tag{2}$$

(2) means that the tire load is determined by vehicle parameters (m,h,l_r,d_l,etc.) and vehicle behavior (Acc_x,Acc_y,Acc_z,ω_p,ω_r). Among these, the term of mg represents the load distribution by vehicle mass, and the terms of Axx_x and Acc_y represent the load transfer by the longitudinal and lateral behavior of the vehicle. The term of Acc_z represents the tire load change due to the road surface and the terms of $\dot{\omega}_p$ and $\dot{\omega}_r$ represent the load transfer due to pitch/roll dynamics. Acc_z is generated in the form of random noise by the road surface and has a much smaller value than Acc_x and Acc_y during normal driving [34]. In addition, since the proposed algorithm aims at a normal driving scenario, pitch/roll dynamics can be assumed to be in steady states [35]. In conclusion, the load transfer dynamics model was derived using the following assumptions.

- Model assumptions : Ignore road surface effect ($Acc_z \approx 0$), steady state pitch/roll dynamics ($\dot{\omega}_p \approx 0, \dot{\omega}_r \approx 0$).

$$\begin{aligned}
F_{Z,FR} + F_{Z,FL} &= mg\left(\frac{l_r}{L} - \frac{h}{L}\frac{Acc_x}{g}\right) \\
F_{Z,RR} + F_{Z,RL} &= mg\left(\frac{l_f}{L} + \frac{h}{L}\frac{Acc_x}{g}\right) \\
F_{Z,FR} + F_{Z,RR} &= mg\left(\frac{d_l}{D} + \frac{h}{D}\frac{Acc_y}{g}\right) \\
F_{Z,FL} + F_{Z,RL} &= mg\left(\frac{d_r}{D} - \frac{h}{D}\frac{Acc_y}{g}\right)
\end{aligned} \tag{3}$$

With the assumptions mentioned about (2) can be converted to (3). It has the same meaning as the analysis of load movement through the side view half-car model in the longitudinal behavior and the front view half-car model in the lateral behavior as shown in Fig. 2. The linear load transfer model represents the relationship of input (Acc_x, Acc_y) to output ($F_{Z,FR}, F_{Z,FL}, F_{Z,RR}, F_{Z,RL}$). The relationship between input and output is determined by vehicle parameters(m, h, l_r, l_f, d_l, d_r). Finally, (3) can be expressed in Multi Input Multi Output(MIMO) system as shown in (4) below.

$$Y = B_0 + B_1 X$$

$$where, X = \begin{bmatrix} Acc_x \\ Acc_y \end{bmatrix}, Y = \begin{bmatrix} F_{Z,FR} + F_{Z,FL} \\ F_{Z,RR} + F_{Z,RL} \\ F_{Z,FR} + F_{Z,RR} \\ F_{Z,FL} + F_{Z,RL} \end{bmatrix}, \quad (4)$$

$$B_0 = \begin{bmatrix} mg\frac{l_r}{L} \\ mg\left(1 - \frac{l_r}{L}\right) \\ mg\frac{d_l}{D} \\ mg\left(1 - \frac{d_l}{D}\right) \end{bmatrix}, B_1 = \begin{bmatrix} -\frac{mh}{L} & 0 \\ \frac{mh}{L} & 0 \\ 0 & \frac{mh}{D} \\ 0 & -\frac{mh}{D} \end{bmatrix}$$

In (4), B_0 and B_1 are composed of vehicle parameters, which are to be estimated in this paper. Acc_x and Acc_y corresponding to input(X) can be measured through the vehicle's IMU sensor. In addition, the tire load corresponding to the output (Y) can be estimated through the intelligent tire. In Section III, we introduce the tire load estimation algorithm using intelligent tire.

III. TIRE LOAD ESTIMATION ALGORITHM USING INTELLIGENT TIRE

A. A Strategy for Estimation of Tire Load

The load applied to the tire is a dominant parameter for the deformation of the tire. Fig. 3 shows the deformation of the tire for heavy and light load, which are realized by the flexible ring tire model. The black line shows the deformation under heavy load and the gray line shows the deformation under light load. As shown in Fig. 4 the tire is deformed more as the load increases and the shape of the longitudinal acceleration of the intelligent tire changes.

For this physical phenomenon, contact length and contact angle are defined as shown in Fig.3. Contact length is the length of the section where the tire and the ground contact with each other and contact angle is the angle of the contact length. The contact angle tends to increase as the load increases. In addition, the lower the tire pressure is, the greater the tire deforms and the longer the contact angle becomes. Therefore, it can be expected that the contact angle is a factor which increases under heavier load and lower tire pressure. In conclusion, we can propose a strategy for estimating the tire load using the characteristics of contact angle. Load applied to the tire is expressed as a function of the contact length and the tire pressure as shown in (5) and (6). However, such strategy requires physical verification. Therefore, such estimation strategy is verified by using a flexible ring tire model in this study.

$$F_z = f_{z1}(p_0, \text{Contact length}(C.L)) \quad (5)$$

$$F_z = f_{z2}(p_0, \text{Contact angle}(\theta_r)) \quad (6)$$

B. Verification by Using Flexible Ring Tire Model

The flexible ring tire model is a very useful tire model in analyzing the radial and longitudinal deformation inside of the tire [32], [36]. The tire load estimation strategy's generality and robustness are verified in this section using the flexible ring tire model.

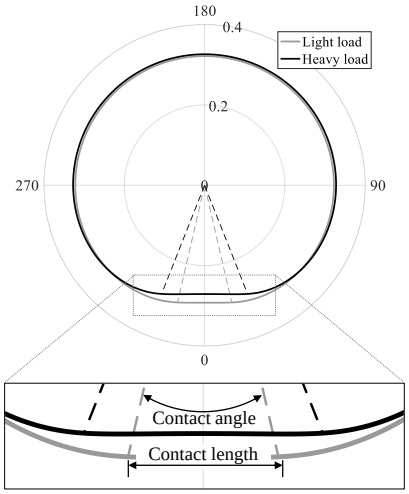

Fig. 3. Contact angle variation due to tire load

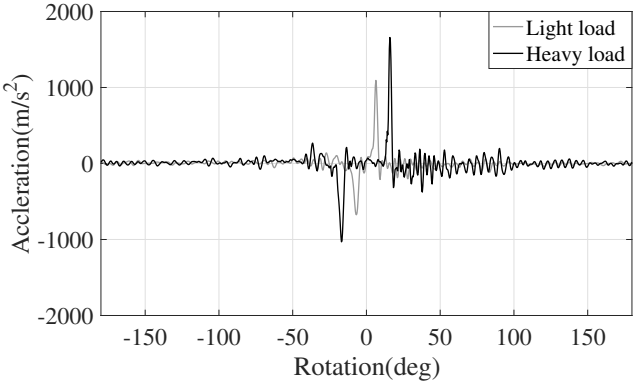

Fig. 4. Longitudinal acceleration variation due to tire load

TABLE III
FLEXIBLE RING TIRE MODEL PARAMETER

Symbol	Parameter	Unit
w	Radial displacement of ring	m
v	Tangential displacement of ring	m
R	Mean radius of side wall	m
k_w	Radial stiffness of sidewall	N/m^2
k_v	Tangential stiffness of sidewall	N/m^2
h	Thickness of the ring	m
b	Width of the ring	m
E	Young's modulus of ring	N/m^2
A	Cross section area of ring	m^2
I	Inertia moment of cross section of ring	m^4
q_w	External force acting on the ring radially	N/m
q_v	External force acting on the ring tangentially	N/m

The following equations are the governing equations of the flexible ring tire model that describes the radial and longitudinal deformation inside of the tire. w represents radial deformation and v represents longitudinal deformation inside of the tire. Since (7) and (8) are fourth order differential equations and coupled to each other, there are many difficulties in solving them. Therefore, the governing equations are summed

up by the following assumptions.

$$\frac{EI}{R^4}\left(\frac{\partial^4 w}{\partial\theta^4}-\frac{\partial^3 v}{\partial\theta^3}\right)+\frac{EA}{R^2}\left(w+\frac{\partial v}{\partial\theta}\right)+\frac{\sigma_\theta^0 A}{R^2}\left(\frac{\partial v}{\partial\theta}-\frac{\partial^2 w}{\partial\theta^2}\right)+k_w w+\rho A(\ddot{w}-2\Omega\dot{v}-\Omega^2 w)-\frac{p_0 b}{R}\left(\frac{\partial v}{\partial\theta}+w\right)=q_w \tag{7}$$

$$\frac{EI}{R^4}\left(\frac{\partial^3 w}{\partial\theta^3}-\frac{\partial^2 v}{\partial\theta^2}\right)+\frac{EA}{R^2}\left(\frac{\partial w}{\partial\theta}+\frac{\partial^2 v}{\partial\theta^2}\right)+\frac{\sigma_\theta^0 A}{R^2}\left(v-\frac{\partial w}{\partial\theta}\right)+k_v v+\rho A(\ddot{v}+2\Omega\dot{w}-\Omega^2 v)+\frac{p_0 b}{R}\left(\frac{\partial w}{\partial\theta}-w\right)=q_v \tag{8}$$

- In-extensibility assumption : The central circumference length of the tire ring does not change.

This assumption has been proved to be reasonable in previous studies of flexible ring tire models [32]. Through the in-extensibility assumption, the relationship between the radial deformation and the longitudinal deformation within the tire can be written as below equation (9).

$$w=-\frac{\partial v}{\partial\theta} \tag{9}$$

Substituting the (9) into (7) and (8), the governing equations are expressed as follows.

$$\frac{EI}{R^4}\left(\frac{\partial^4 w}{\partial\theta^4}-\frac{\partial^3 v}{\partial\theta^3}\right)+\frac{\sigma_\theta^0 A}{R^2}\left(\frac{\partial v}{\partial\theta}-\frac{\partial^2 w}{\partial\theta^2}\right)+k_w w+2A\Omega^2 w=q_w \tag{10}$$

$$\frac{EI}{R^4}\left(\frac{\partial^3 w}{\partial\theta^3}-\frac{\partial^2 v}{\partial\theta^2}\right)+\frac{\sigma_\theta^0 A}{R^2}\left(v-\frac{\partial w}{\partial\theta}\right)+k_v v-2A\Omega^2 v+\frac{p_0 b}{R}\left(\frac{\partial w}{\partial\theta}-w\right)=q_v \tag{11}$$

When subtracting the differential (11) for theta from (10) and applying in-extensibility assumption, it is expressed as (12) below.

Differentiating (11) by θ and subtracting it with (10) yields the following equation.

$$-\frac{p_0 b}{R}\frac{\partial^2 w}{\partial\theta^2}+\left(k_w+k_v-\frac{p_0 b}{R}\right)w=q_w-\frac{\partial q_v}{\partial\theta} \tag{12}$$

It can be noticed that the radial deformation inside of the tire has the same behavior as the mass-spring system where the force is expressed by the radial and longitudinal forces received from the ground. The total load which tire is receiving from the ground is:

$$F_z=R\int q_w\cos\theta d\theta \tag{13}$$

In addition, free rolling assumption($q_v=0$) and geometric assumption was used [37], [38].

- Geometrical assumption : Tires move on frictionless, flat surfaces

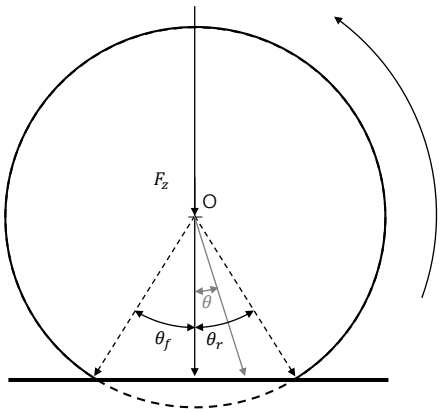

Fig. 5. Geometrical assumption

Fig. 5 illustrates the behavior of a tire under geometric assumptions. θ_r is the rear contact angle. Since the damping effect of the tire is not considered in this study, the front contact angle (θ_f) is equal to the real contact angle(θ_r). That is, $\theta_f=-\theta_r$. The radial deformation within the tire under the geometric assumption is as follows

$$w(\theta)=\begin{cases}R\left(1-\frac{cos(\theta_r)}{cos(\theta)}\right) & \text{if } \theta_f<\theta<\theta_r\\ 0 & \text{otherwise}\end{cases} \tag{14}$$

Finally, the following equation can be obtained by combining (12) and (13) obtained from in-extensibility assumption and (14) obtained from geometric assumption.

$$F_z=2Rp_0 b\sin\theta r+2R^2(k_w+k_v)(\sin\theta r-\theta r\cos\theta r) \tag{15}$$

The relation above has the following meaning. First, the contact angle increases when tire load increases. Second, for the same contact angle, higher tire pressure means heavier tire load. Moreover, the tire load is not affected by the wheel rotational speed, tire wear, etc. and is dominated by contact angle and tire pressure. In conclusion, (15) verifies the tire load estimation strategy shown as Fig. 3. In other words, the tire load can be expressed as a function of contact angle and tire pressure as shown in Equation 3.10. Therefore, it is proved that the load could be estimated if the contact angle and tire pressure are known. In the case of tire pressure, it is a value that can be measured directly. In the case of contact angle, the contact angle can be estimated through an intelligent tire sensor signal which is shown in the next section. In conclusion, tire load is estimated based on the measured tire pressure and estimated contact angle.

C. Estimation of Contact Angle Using Intelligent Tires

According to the previous intelligent tire research, the contact angle between the tire and the road surface has been estimated in two ways. One is the method based on longitudinal acceleration [24], [23] the other is the method based on radial jerk [25]. In this paper, a method for estimating the

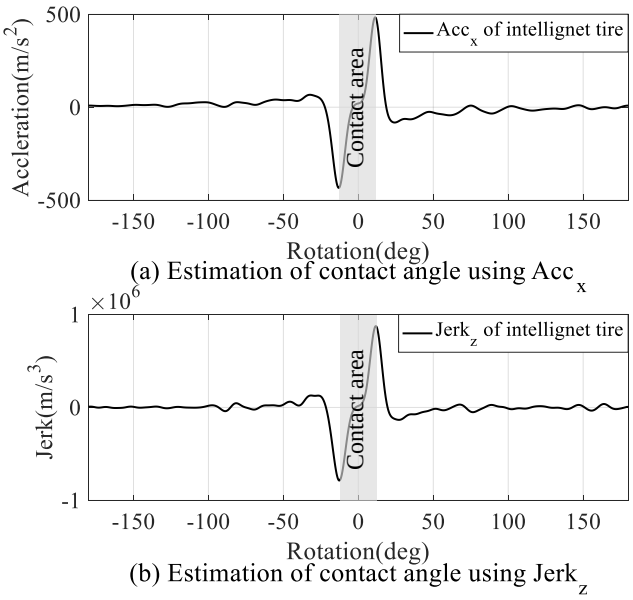

Fig. 6. Two algorithms for estimating contact angle

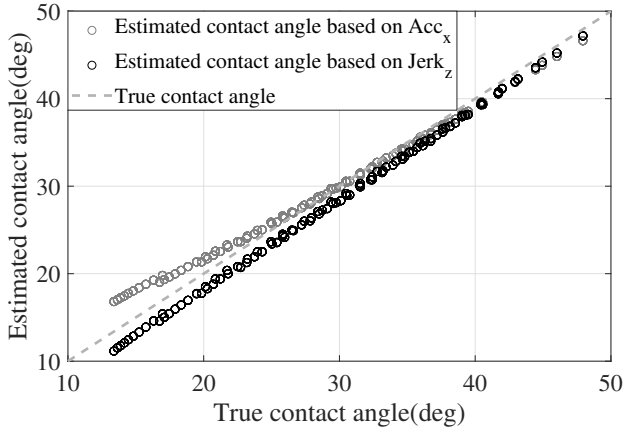

Fig. 7. Verification of estimation algorithm using flexible ring tire model

TABLE IV
TIRE CONDITIONS OF FLEXIBLE RING TIRE MODEL SIMULATION

Tire condition	Value
Tire load	2000N ~ 10000N, 10 levels
Velocity	30km/h ~ 100km/h, 10 levels
Pressure	1.0bar ~ 2.4 bar, 10 levels

contact angle which combines the two methods is proposed. In this chapter, the estimation method based on the longitudinal acceleration and the estimation method based on the radial jerk were verified by the flexible ring tire model.

First, the contact angle estimation algorithm based on longitudinal acceleration is as follows. The contact angle is defined as the angle between the maximum and minimum points of longitudinal acceleration, as shown in Fig. 6(a). This has the following physical meanings. At the start of the tire-to-road contact, momentary force is exerted, so the longitudinal acceleration is at its maximum. In addition, the tire will release momentarily at the end of the tire and road contact, so the magnitude of longitudinal acceleration will be maximum.

Second, the contact angle estimation algorithm based on the radial jerk is as follows. The contact angle between the tire and the road surface is defined as the angle between the maximum and minimum points of the radial jerk, which is the differential form of the radial acceleration as shown in Fig. 6 (b). This is explained similar to the physical analysis of longitudinal acceleration described above. That is, the radial force applied to the tire at the start and the end of the contact between the tire and the road surface instantly becomes zero, and the amount of change is maximum. Therefore, it can be seen that this will maximize the radial jerk value at the boundary of the tire and road contact.

Each contact angle estimation algorithms mentioned above was verified by using flexible ring tire model. The verification was performed by comparing the actual contact angle obtained from the flexible ring tire model with the estimated contact angle based on the longitudinal and radial acceleration. In this case, a total of 1000 conditions (10 pressure stages * 10 speed stages * 10 load stages) were used in the analysis, and each condition is shown in Table IV.

The simulation results are shown in Fig. 7. The x-axis is the actual contact angle obtained from the flexible ring tire model, and the y-axis is the contact angle estimated based on the longitudinal and radial acceleration. It is confirmed that the actual contact angle and the estimated contact angle had a linear relationship. This means that the contact angle estimated by the two algorithms are reasonable.

According to the analysis done by using flexible ring tire model, the real contact angle has a value between the contact angle estimated based on the longitudinal acceleration($Acc_x \approx \ddot{v}$) and the contact angle estimated based on the radial jerk($Jerk_z \approx \dddot{w}$). As a result, the contact angle was estimated by the weighted sum of the contact angles estimated in each way.

The weight, w, can be defined more exquisitely by an experiment that measures the actual contact angle of the tire. In this paper, the weight is set to 1/2. In conclusion, in this paper, the ground angle between the tire and the road surface was estimated as follows.

$$\begin{aligned} \hat{CL} &= w \times CL(\hat{Acc}_x) + (1-\lambda) \times CL(\hat{Jerk}_z) \\ \text{where} \hat{CL} &= \text{Estimated contact angle} \\ CL(\hat{Acc}_x) &= \text{Estimated contact angle based on} Acc_x \\ CL(\hat{Jerk}_z) &= \text{Estimated contact angle based on} Jerk_z \\ \lambda &= \text{weight factor} \end{aligned} \tag{16}$$

$$\hat{CL} = \frac{CL(\hat{Acc}_x) + CL(\hat{Jerk}_z)}{2} \tag{17}$$

D. Estimation of Tire Load Using Intelligent Tires

According to the analysis mentioned above, tire load can be expressed as a function of contact angle and tire pressure. In

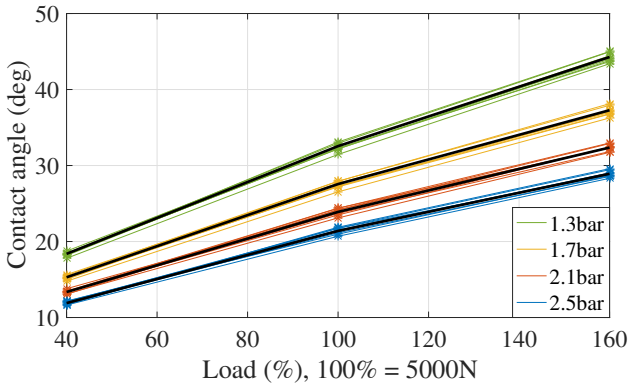

Fig. 8. Relationship between load, contact angle and pressure

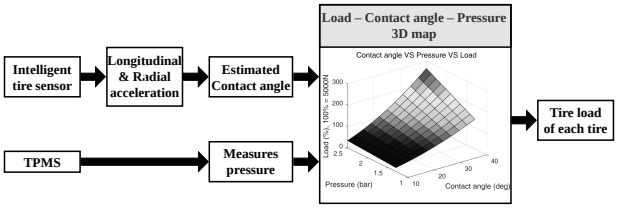

Fig. 9. Schematic of load estimation algorithm using intelligent tire

TABLE V
RMS ERROR OF LOAD ESTIMATION USING INTELLIGENT TIRE (%)

30km/h/65km/h	40% load	100% load	160% load
1.3bar	1.53% / 1.12%	1.06% / 1.29%	0.58% / 1.51%
1.7bar	0.82% / 2.36%	2.36% / 1.12%	0.40% / 0.80%
2.1bar	1.93% / 2.42%	1.02% / 1.58%	0.86% / 1.45%
2.5bar	1.93% / 3.79%	1.02% / 1.19%	0.86% / 1.17%

this section, a three-dimensional map of load-contact angle-tire pressure is constructed based on intelligent tire sensor signals obtained by an experiment using a Flat trac. In this case, the contact angle was estimated using an intelligent tire sensor signal.

Fig. 8 is a graph of load-contact angle-tire pressure under the conditions shown in Table. I . The x-axis is the tire load where load at 100% is 5000N and the y-axis is the contact angle. Each color represents the relationship between load and contact angle for each pressure. The graph of each pressure is slightly dispersed by speed and wear. A total of 12 conditions (speed 3 stages * wear 4 stages) are included for one pressure. The solid black line represents the average of the tire load and contact angle at each pressure.

As shown in Fig. 8, the tire load is very dominant in contact angle and tire pressure. In contrast, speed and wear do not significantly affect the tire load. In conclusion, similar to the analysis using flexible ring tire model, it is verified that the tire load can be expressed as a function of contact angle and tire pressure. The tire load is estimated by the algorithm shown in Fig. 9. First, tire pressure and estimated contact angle are the inputs of the estimator. Then, the load applied to the tire is output estimated by the load-contact angle-tire pressure map made previously by an indoor experiment.

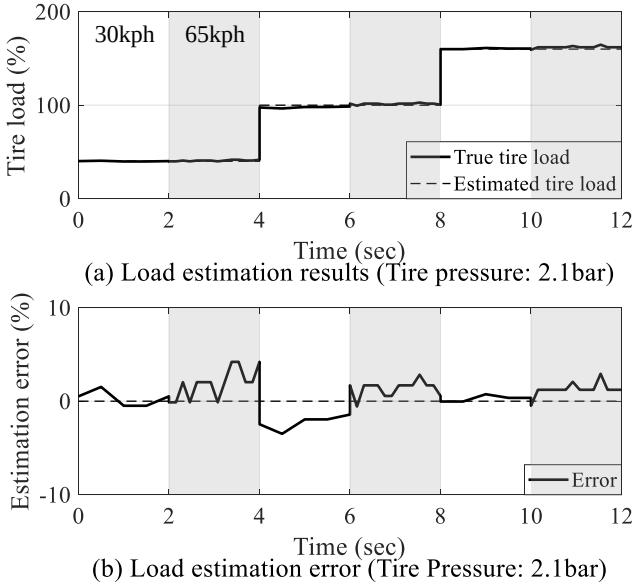

Fig. 10. Performance of load estimation algorithm using intelligent tire

An indoor test of the tire load estimation method was conducted with a 2.9 mm worn tire. The tires were tested under the conditions shown in Table. I, and each experiment was conducted for 2 seconds. After that, the tire load was estimated using the intelligent tire sensor signal and load-contact angle-tire pressure map obtained from the indoor experiment. Then, actual tire loads and the loads estimated by the proposed algorithm are compared. Fig. 10 shows the load estimation performance for 2.1 bar pressure condition. Table. V show the load estimation performance for various pressures. The error is within 5% under all conditions and shows high estimation performance.

IV. VEHICLE PARAMETER ESTIMATION AND TIRE LOAD COMPENSATION ALGORITHM

In this section, we propose a vehicle parameter estimation algorithm and tire load compensation algorithm based on vehicle dynamics. The estimation of tire load by intelligent tire alone has the following limitations. First, the load estimated by the intelligent tire has a low sampling rate. Due to the procedure of the algorithm, the tire load is estimated once per wheel. This has a limitation that it is not possible to properly estimate a tire load in a severe driving situation where tire load is changed rapidly. Second, it has low robustness in estimating tire load under driving conditions with acceleration, deceleration and steering. Therefore, this paper tries to solve those limitations by combining with the vehicle dynamics model.

The combination with the vehicle dynamics model has the following advantages. First, a high sampling rate can be obtained. The IMU sensor of the vehicle has a sampling rate of 100 Hz, allowing fast tire load estimation. Second, high robustness is guaranteed compared to the load estimation algorithm where intelligent tires are used alone. Finally, CG point and

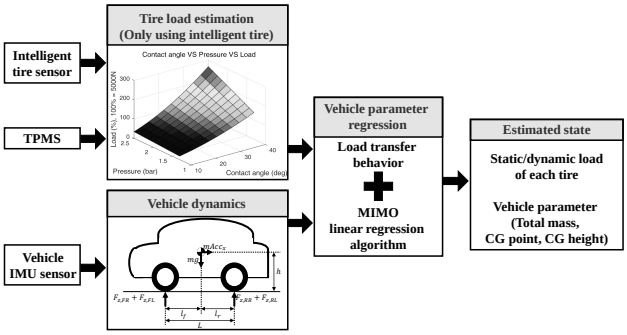

Fig. 11. Schematic of proposed estimation algorithm

CG height can be estimated by combining with the vehicle dynamics model. Estimation of such vehicle parameters is expected to contribute greatly in the field of vehicle control.

A. MIMO Linear Regression Algorithm

This section proposes an algorithm for estimating vehicle weight (m), CG point (l_r, d_l), and CG height (h) based on the vehicle dynamics model analyzed above. In (4), we proved that the load transfer model can be expressed as a MIMO system. The longitudinal/lateral acceleration corresponding to X can be measured by the vehicle's IMU sensor, and each wheel load corresponding to Y can be estimated using the tire load estimation algorithm proposed in chapter III. Finally, MIMO linear regression algorithm was used to estimate the vehicle parameters expressed as B_0 and B_1 [39].

The MIMO linear regression algorithm finds vehicle parameters that minimize a cost function such as (18). The cost function consists of the sum of squares of each parameter error.

$$J = \Sigma \left(Y - (B_0 + B_1 X)\right)' \left(Y - (B_0 + B_1 X)\right) \tag{18}$$

Finally, the vehicle parameters were estimated to minimize the cost function(J).

$$\hat{m}, \hat{l_r}, \hat{d_l}, \hat{h} = argmin_{m,l_r,d_l,h} J \tag{19}$$

The estimated value of each parameter can be expressed as follows.

$$\begin{aligned}
\hat{m} &= \frac{\bar{y1} + \bar{y2} + \bar{y3} + \bar{y4}}{4} \\
\hat{h} &= \frac{-DS_{x1y1} + DS_{x1y2} + LS_{x2y3} - LS_{x2y4}}{\frac{\hat{m}D}{L} S_{x1x1} + \frac{\hat{m}L}{D} S_{x2x2}} \\
\hat{l_r} &= L \times \left(\frac{1}{2} + \frac{\bar{y1} - \bar{y2}}{2\hat{m}g} + \frac{\hat{h}}{L} \frac{\bar{x1}}{g} \right) \\
\hat{d_l} &= D \times \left(\frac{1}{2} + \frac{\bar{y3} - \bar{y4}}{2\hat{m}g} - \frac{\hat{h}}{D} \frac{\bar{x2}}{g} \right) \\
&\text{where, } x1 = Acc_x, x2 = Acc_y \\
y1 &= F_{Z,FR} + F_{Z,FL}, y2 = F_{Z,RR} + F_{Z,RL}, \\
y3 &= F_{Z,FR} + F_{Z,RR}, y4 = F_{Z,FL} + F_{Z,RL}, \\
\bar{xi} &= \frac{\Sigma xi}{n}, S_{xiyi} = \frac{\Sigma xiyi}{n} - \bar{xi}\bar{yi}
\end{aligned} \tag{20}$$

TABLE VI
REFERENCE OF VEHICLE PARAMETERS

Vehicle parameters	Value
m	1579kg
l_r	1.510m
d_l	0.753m
h	0.535m

(20) shows how to estimate vehicle parameters based on longitudinal/lateral acceleration measured by IMU of vehicle and estimated load by intelligent tire sensor. In conclusion, it can be confirmed that vehicle parameters such as total mass, CG point, and CG height can be estimated using the vehicle dynamics model. Through this equation, the total mass and CG point can be estimated for all driving conditions, but the CG height can be estimated only when there is a load transfer. In addition, by using estimated vehicle parameter and (3), the static/dynamic load of each tire can be estimated.

The proposed vehicle parameter and tire load estimation algorithm are constructed as shown in Fig. 11. Intelligent tire sensors, vehicle's IMU sensors were used. In order to estimate the vehicle parameters and tire load is first estimated using intelligent tire at low sampling rate. Finally, static/dynamic load of each tire and the vehicle parameters are estimated by vehicle dynamics and MIMO L-r algorithm.

B. Experiment configuration and scenario

The performance of the proposed estimation algorithm is verified by real vehicle test. Measurements are each wheel intelligent tire sensor signal and vehicle IMU sensor signal. The experiment used Autobox III for real time experiments. Autobox III received the sensor signal and implemented the estimation algorithm. The Hyundai i30 vehicle was used for the experiment. The specifications of the vehicle are shown in Table. VI. For tires, the all season tire 195/65R15 was used. The proposed tire load and vehicle parameter estimation algorithm is implemented through Simulink.

Real vehicle experiments consist of three scenarios. The first is a straight constant driving scenario, the second is an acceleration/deceleration driving scenario and the third is a general driving scenario with longitudinal/lateral acceleration. Scenarios are situations that occur frequently in real driving. Therefore, the proposed tire load and vehicle parameter estimation algorithm is verified for the above three experimental scenarios. In each experiment, all four wheels used the same tire, and the pressure and load of each wheel were set differently.

The estimated values are static/dynamic load of each load, CG point and CG height. For the static load of each tire, CG point and CG height, the actual values were used for the accuracy verification. For each wheel dynamic load, the actual value could not be measured, so each wheel load calculated from (3) based on the actual vehicle specification and acceleration was used for the accuracy verification.

V. RESULTS

Estimated static/dynamic tire load and vehicle parameter estimated by the intelligent tire sensor and the vehicle's IMU

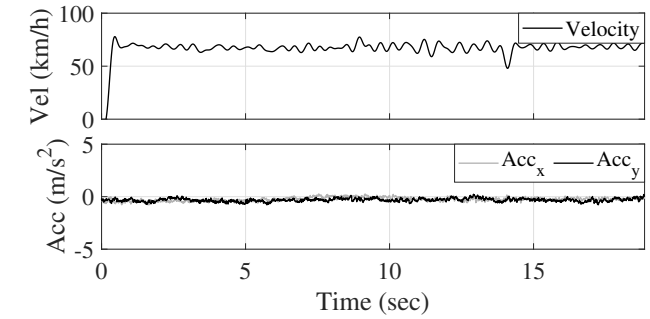

(a) Velocity and longitudinal/lateral acceleration

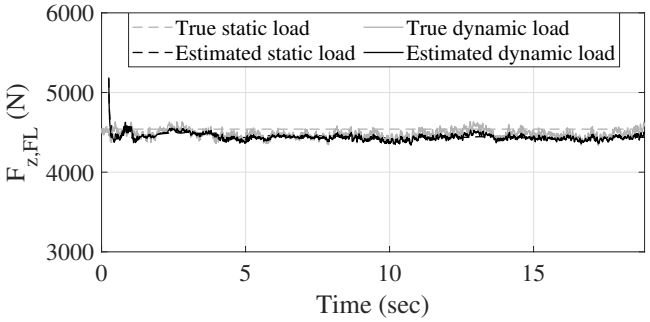

(b) Estimation of tire static/dynamic load

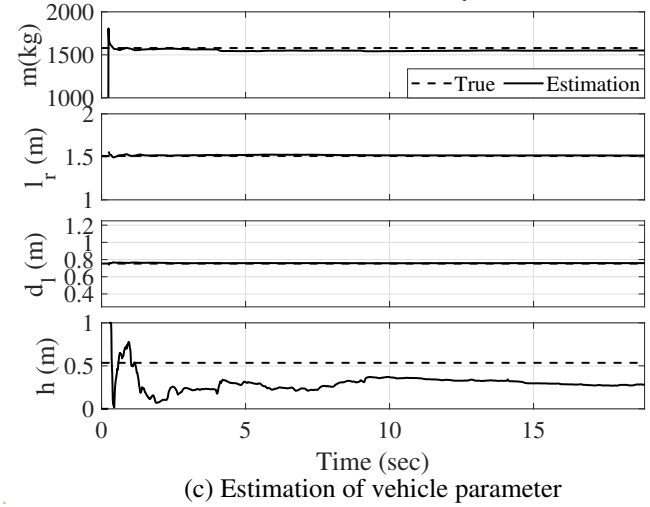

(c) Estimation of vehicle parameter

Fig. 12. Scenario 1: Real-time experiment results

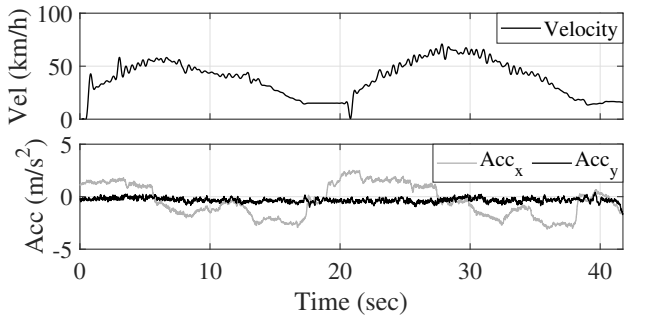

(a) Velocity and longitudinal/lateral acceleration

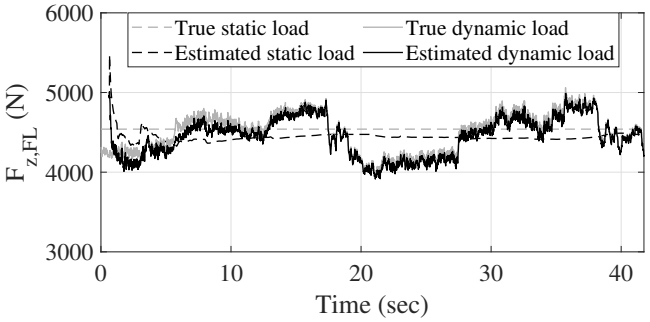

(b) Estimation of tire static/dynamic load

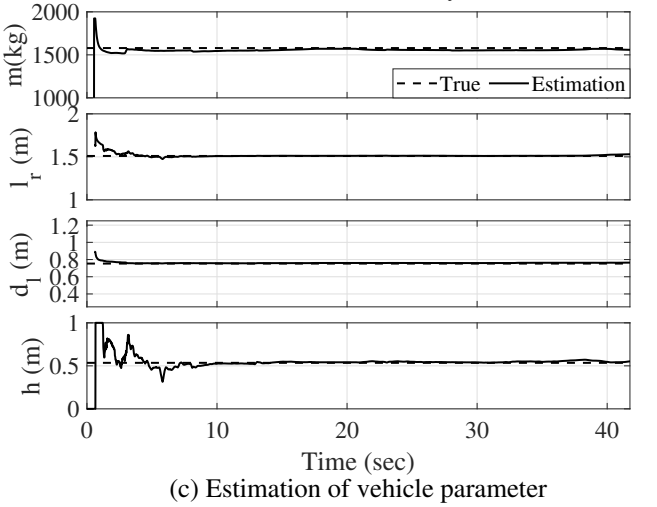

(c) Estimation of vehicle parameter

Fig. 13. Scenario 2: Real-time experiment results

sensor for each scenario are as follows.

A. Scenario 1: Straight and Constant Velocity

The estimated tire static/dynamic tire load and vehicle parameters for the constant speed driving situation are shown in Fig. 12, and the estimation performance is shown in Table. VII. In constant velocity, the speed of the vehicle is constant and no load transfer occurs because there is no longitudinal/lateral acceleration. Therefore, the CG height cannot be estimated in the straight constant velocity situation. Total mass and CG point excluding CG height were estimated to be around 2.5% error. In addition, after the estimation of the vehicle parameters is completed, the static/dynamic tire load showed the performance within the error 3.5%Ṡince there is no load transfer, the estimated values converge quickly.

B. Scenario 2: Acceleration and Deceleration

For the straight acceleration/deceleration driving, experiments were performed by setting 20 80km/h speed and –0.3g +0.3g longitudinal acceleration as shown in Fig. 13(a). The estimated static/dynamic tire load and vehicle parameters are shown in Fig. 13(b), (c), and the estimation performance is shown in Table. VIII. In case of the straight acceleration/deceleration, there is a load transfer to the front and rear of the vehicle. Therefore, unlike the scenario 1, the CG height is also estimated. Vehicle parameter estimation shows a performance of around 1.5% error. After estimating the vehicle parameters, it was confirmed that the tire dynamic load estimation has a fast sampling rate. In addition, the static tire load and vehicle parameters of the vehicle converged to the true value even during the acceleration and deceleration. This means that high robustness is achieved through the

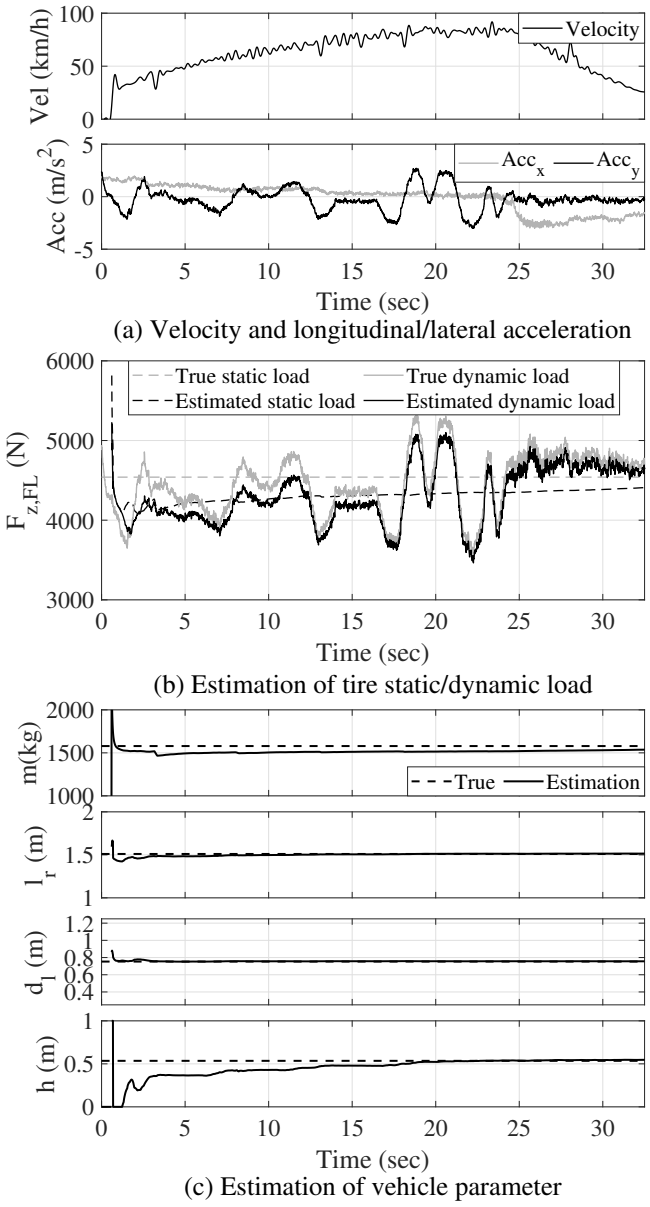

Fig. 14. Scenario 3: Real-time experiment results

combination of vehicle dynamics. Estimation of static/dynamic tire load shows a performance of around 3.5% error. The estimation time is 20sec, which is longer than the scenario 1 because the CG height is also estimated.

C. Scenario 3: Longitudinal/Lateral Acceleration

For the last scenario, it is suggested to describe the driving situation in general. Scenario 3 is a driving situation in which the longitudinal acceleration is between -0.3g and +0.3g and the lateral acceleration is between and -0.3g and +0.3g, as shown in Fig.14(a). The estimated values are shown in Fig. 14(b), (c) and the accuracy is shown in Table. IX.For scenario 3 with longitudinal and lateral acceleration, it was also verified that the static/dynamic tire load and the vehicle parameters converged to true as in Fig. 14(c). This confirms that the proposed algorithm is robust under normal driving conditions.

TABLE VII
SCENARIO 1: RMS ERROR OF ESTIMATED PARAMETER AND LOAD

Vehicle parameters		Static load / Dynamic load of each tire	
m	2.260%	$F_{Z,FR}$	0.871% / 3.505%
l_r	0.762%	$F_{Z,FL}$	2.184% / 1.199%
d_l	0.666%	$F_{Z,RR}$	2.240% / 3.200%
h	-	$F_{Z,RL}$	3.364% / 1.004%

TABLE VIII
SCENARIO 2: RMS ERROR OF ESTIMATED PARAMETER AND LOAD

Vehicle parameters		Static load / Dynamic load of each tire	
m	0.538%	$F_{Z,FR}$	0.712% / 3.416%
l_r	0.094%	$F_{Z,FL}$	2.268% / 2.438%
d_l	0.920%	$F_{Z,RR}$	0.873% / 2.531%
h	1.124%	$F_{Z,RL}$	2.670% / 2.068%

TABLE IX
SCENARIO 3: RMS ERROR OF ESTIMATED PARAMETER AND LOAD

Vehicle parameters		Static load / Dynamic load of each tire	
m	4.084%	$F_{Z,FR}$	2.918% / 5.822%
l_r	0.091%	$F_{Z,FL}$	3.884% / 3.880%
d_l	0.529%	$F_{Z,RR}$	3.456% / 4.822%
h	2.307%	$F_{Z,RL}$	4.225% / 3.185%

In addition, as in the previous scenarios, tire dynamic load estimation has a fast sampling rate after vehicle parameter estimation. In the case of scenario 3, the estimated static/dynamic tire load accuracy showed an error of about 4% and the vehicle parameter accuracy showed an error of about 6%.The estimated time was 21sec, which is similar to scenario 2.

Experimental results show that the proposed algorithm has the following advantages. First, each static/dynamic tire load and vehicle parameters can be estimated based on the proposed algorithm. The estimated static/dynamic tire load and vehicle parameters are expected to be actively used in various fields including vehicle control. In addition, the estimation accuracy showed a performance of around 5% error. Second, the dynamic load of each tire can be estimated at a sampling rate of 100 Hz. This is a very fast estimation speed compared to estimating tire load using only intelligent tire sensor. Third, by combining with vehicle dynamics, it is possible to estimate static/dynamic tire load and vehicle parameters even when the vehicle has longitudinal/lateral behavior. This means that the proposed estimation algorithm has high robustness.

VI. CONCLUSION AND FUTURE WORK

In this paper, an algorithm for the estimation of tire static/dynamic load and vehicle parameters using intelligent tires and vehicle dynamics was proposed. A tire load estimation algorithm was proposed using intelligent tires. The proposed load estimation method was verified by the flexible ring tire model. But using such algorithm alone has the limitation of low sampling rate and low robustness. To overcome this, we proposed a tire load compensation algorithm that combines intelligent tires and vehicle dynamics. The linear load transfer model was used as a vehicle dynamics model. Finally, tire static/dynamic load and vehicle parameters can be estimated using a multi-input multi-output (MIMO) linear

regression algorithm. As a result, the proposed algorithm has a faster sampling rate and high robustness in estimating tire load compared to the tire load estimation using intelligent tire alone. Also, vehicle parameters such as total mass, CG points, and CG height can be estimated by the proposed algorithm. Incorrect vehicle parameters adversely affect vehicle control performance. But, there was a problem that there was no system capable of accurately measuring vehicle parameters in real-time. The proposed estimation algorithm provides more accurate vehicle parameters. In conclusion, the proposed algorithm is expected to contribute in the field of vehicle control and measurement. The limitations and future work of this study are as follows. First, the proposed estimation algorithm used a simple vehicle model that does not consider air resistance or road surface profile. Analysis of slope, bank, drag force, etc. is required for precise performance verification. Second, the performance of the estimated dynamic tire load was analyzed through a comparison with the vehicle dynamics model. In the future, performance verification using wheel force transducers is required.

ACKNOWLEDGMENT

This research was partly supported by the Industrial Strategic Technology Development Program funded by the HANKOOK TIRE CO.LTD. and the BK21+ program through the NRF funded by the Ministry of Education of Korea.

REFERENCES

[1] H. Zhang and J. Wang, "Vehicle lateral dynamics control through afs/dyc and robust gain-scheduling approach," *IEEE Transactions on Vehicular Technology*, vol. 65, no. 1, pp. 489–494, 2015.

[2] C. Zhao, W. Xiang, and P. Richardson, "Vehicle lateral control and yaw stability control through differential braking," in *2006 IEEE international symposium on industrial electronics*, vol. 1. IEEE, 2006, pp. 384–389.

[3] Z. Yong, S. Jian, W. Di, and X. Chunxin, "Automatic transmission shift point control under different driving vehicle mass," SAE Technical Paper, Tech. Rep., 2002.

[4] J. Song, H. Kim, and K. Boo, "A study on an anti-lock braking system controller and rear-wheel controller to enhance vehicle lateral stability," *Proceedings of the Institution of Mechanical Engineers, Part D: Journal of Automobile Engineering*, vol. 221, no. 7, pp. 777–787, 2007.

[5] M. N. Mahyuddin, J. Na, G. Herrmann, X. Ren, and P. Barber, "Adaptive observer-based parameter estimation with application to road gradient and vehicle mass estimation," *IEEE Transactions on Industrial Electronics*, vol. 61, no. 6, pp. 2851–2863, 2013.

[6] A. Vahidi, M. Druzhinina, A. Stefanopoulou, and H. Peng, "Simultaneous mass and time-varying grade estimation for heavy-duty vehicles," in *Proceedings of the 2003 American Control Conference, 2003.*, vol. 6. IEEE, 2003, pp. 4951–4956.

[7] P. Lingman and B. Schmidtbauer, "Road slope and vehicle mass estimation using kalman filtering," *Vehicle System Dynamics*, vol. 37, no. sup1, pp. 12–23, 2002.

[8] H. K. Fathy, D. Kang, and J. L. Stein, "Online vehicle mass estimation using recursive least squares and supervisory data extraction," in *2008 American control conference*. IEEE, 2008, pp. 1842–1848.

[9] A. Vahidi, A. Stefanopoulou, and H. Peng, "Recursive least squares with forgetting for online estimation of vehicle mass and road grade: theory and experiments," *Vehicle System Dynamics*, vol. 43, no. 1, pp. 31–55, 2005.

[10] M. Doumiati, A. Victorino, A. Charara, and D. Lechner, "Lateral load transfer and normal forces estimation for vehicle safety: experimental test," *Vehicle System Dynamics*, vol. 47, no. 12, pp. 1511–1533, 2009.

[11] Y. Cui and T. R. Kurfess, "Vehicle parameter identification for vertical dynamics," *Journal of Dynamic Systems, Measurement, and Control*, vol. 137, no. 2, 2015.

[12] B. Li, J. Zhang, H. Du, and W. Li, "Two-layer structure based adaptive estimation for vehicle mass and road slope under longitudinal motion," *Measurement*, vol. 95, pp. 439–455, 2017.

[13] X. Huang and J. Wang, "Longitudinal motion based lightweight vehicle payload parameter real-time estimations," *Journal of Dynamic Systems, Measurement, and Control*, vol. 135, no. 1, 2013.

[14] B. M. Lacquet, P. L. Swart, and A. P. Kotzé, "A low-cost on-board vehicle load monitor," *Measurement Science and Technology*, vol. 7, no. 12, p. 1761, 1996.

[15] M. Q. Feng, R. Y. Leung, and C. M. Eckersley, "Non-contact vehicle weigh-in-motion using computer vision," *Measurement*, vol. 153, p. 107415, 2020.

[16] X. Zhao, H. Jiang, S. Zheng, and J. Han, "Development of high precision gravity center position measurement system for large heavy vehicles," in *ICMIT 2005: Control Systems and Robotics*, vol. 6042. International Society for Optics and Photonics, 2006, p. 604241.

[17] X. Zhang, M. Wang, W. Tang, and J. Wang, "A flexible measurement technique for testing the mass and center of gravity of large-sized objects," *Measurement Science and Technology*, vol. 31, no. 1, p. 015006, 2019.

[18] H. Lee and S. Taheri, "Intelligent tires? a review of tire characterization literature," *IEEE Intelligent Transportation Systems Magazine*, vol. 9, no. 2, pp. 114–135, 2017.

[19] H. Morinaga, "Method for estimating tire wear and apparatus for estimating tire wear," Jul. 9 2013, uS Patent 8,483,976.

[20] Y. Hanatsuka, "Method and apparatus for detecting wear of tire," Nov. 22 2011, uS Patent 8,061,191.

[21] F. Braghin, M. Brusarosco, F. Cheli, A. Cigada, S. Manzoni, and F. Mancosu, "Measurement of contact forces and patch features by means of accelerometers fixed inside the tire to improve future car active control," *Vehicle System Dynamics*, vol. 44, no. sup1, pp. 3–13, 2006.

[22] R. Matsuzaki, N. Hiraoka, A. Todoroki, and Y. Mizutani, "Analysis of applied load estimation using strain for intelligent tires," *Journal of Solid Mechanics and Materials Engineering*, vol. 4, no. 10, pp. 1496–1510, 2010.

[23] D. Jeong, J. Lee, S. Choi, and M. Kim, "Load estimation of intelligent tires equipped with acceleration sensors," in *2019 IEEE Sensors Applications Symposium (SAS)*. IEEE, 2019, pp. 1–5.

[24] A. Niskanen and A. Tuononen, "Three three-axis iepe accelerometers on the inner liner of a tire for finding the tire-road friction potential indicators," *Sensors*, vol. 15, no. 8, pp. 19 251–19 263, 2015.

[25] S. Hong, G. Erdogan, K. Hedrick, and F. Borrelli, "Tyre–road friction coefficient estimation based on tyre sensors and lateral tyre deflection: modelling, simulations and experiments," *Vehicle system dynamics*, vol. 51, no. 5, pp. 627–647, 2013.

[26] G. Erdogan, S. Hong, F. Borrelli, and K. Hedrick, "Tire sensors for the measurement of slip angle and friction coefficient and their use in stability control systems," *SAE International Journal of Passenger Cars-Mechanical Systems*, vol. 4, no. 2011-01-0095, pp. 44–58, 2011.

[27] G. Erdogan, L. Alexander, and R. Rajamani, "A novel wireless piezoelectric tire sensor for the estimation of slip angle," *Measurement Science and Technology*, vol. 21, no. 1, p. 015201, 2009.

[28] S. Kim, K.-S. Kim, and Y.-S. Yoon, "Development of a tire model based on an analysis of tire strain obtained by an intelligent tire system," *International Journal of Automotive Technology*, vol. 16, no. 5, pp. 865–875, 2015.

[29] Y. Xiong and A. Tuononen, "A laser-based sensor system for tire tread deformation measurement," *Measurement Science and Technology*, vol. 25, no. 11, p. 115103, 2014.

[30] J. Yunta, D. Garcia-Pozuelo, V. Diaz, and O. Olatunbosun, "Influence of camber angle on tire tread behavior by an on-board strain-based system for intelligent tires," *Measurement*, vol. 145, pp. 631–639, 2019.

[31] S. Hong and J. K. Hedrick, "Tire-road friction coefficient estimation with vehicle steering," in *2013 IEEE Intelligent Vehicles Symposium (IV)*. IEEE, 2013, pp. 1227–1232.

[32] S. Gong, "Study of in-plane dynamics of tires," 1993.

[33] D. Krier, G. S. Zanardo, and L. del Re, "A pca-based modeling approach for estimation of road-tire forces by in-tire accelerometers," *IFAC Proceedings Volumes*, vol. 47, no. 3, pp. 12 029–12 034, 2014.

[34] E. Velenis, E. Frazzoli, and P. Tsiotras, "On steady-state cornering equilibria for wheeled vehicles with drift," in *Proceedings of the 48h IEEE Conference on Decision and Control (CDC) held jointly with 2009 28th Chinese Control Conference*. IEEE, 2009, pp. 3545–3550.

[35] R. Rajamani, *Vehicle dynamics and control*. Springer Science & Business Media, 2011.

[36] S.-J. Kim and A. R. Savkoor, "The contact problem of in-plane rolling of tires on a flat road," *Vehicle System Dynamics*, vol. 27, no. S1, pp. 189–206, 1997.
[37] Z.-X. Yu, H.-F. Tan, X.-W. Du, and L. Sun, "A simple analysis method for contact deformation of rolling tire," *Vehicle System Dynamics*, vol. 36, no. 6, pp. 435–443, 2001.
[38] A. J. Niskanen, Y. Xiong, and A. J. Tuononen, "Towards the friction potential estimation: A model-based approach to utilizing intyre accelerometer measurements," in *2016 IEEE Intelligent Vehicles Symposium (IV)*. IEEE, 2016, pp. 625–629.
[39] D. Simon, *Optimal state estimation: Kalman, H infinity, and nonlinear approaches*. John Wiley & Sons, 2006.

Dasol Jeong received the B.S. degree in mechanical engineering from Korea Advanced Institute of Science and Technology (KAIST), Deajeon, Korea, and M.S. in Mechanical Engineering from the Korea Advanced Institute of Science and Technology (KAIST), in 2017 and 2019, respectively. Since 2019, he is currently pursuing the Ph.D. degree in Mechanical engineering at KAIST. His research interests include vehicle dynamics and control, intelligent tires, path planning, and control theory.

Seungtaek Kim received the B.S. degree in mechanical engineering from Yonsei University, Seoul, Korea, in 2019. Since 2019, he is currently pursuing the M.S. degree in Mechanical engineering at Korea Advanced Institute of Science and Technology (KAIST). His research interests include intelligent tires, vehicle dynamics and control theory.

Jonghyup Lee received the B.S. degree in mechanical engineering from Korea Advanced Institute of Science and Technology (KAIST), Deajeon, Korea, and M.S. in Mechanical Engineering from the Korea Advanced Institute of Science and Technology (KAIST), in 2015 and 2017, respectively. Since 2019, he is currently pursuing the Ph.D. degree in Mechanical engineering at KAIST. His current research interests include vehicle dynamics and control, intelligent tires and vehicle safety systems.

Seibum B. Choi (M'09) received the B.S. in mechanical engineering from Seoul National University, Seoul, Korea, the M.S. in mechanical engineering from KAIST, Deajeon, Korea, and the Ph.D. in control from the University of California, Berkeley, CA, USA, in 1993. From 1993 to 1997, he was involved in the development of automated vehicle control systems at the Institute of Transportation Studies, University of California. Through 2006, he was with TRW, Livonia, MI, USA, where he was involved in the development of advanced vehicle control systems. Since 2006, he has been faculty in the Mechanical Engineering Department, KAIST, Korea. His current research interests include fuel-saving technology, vehicle dynamics and control, and active safety systems. Prof. Choi is a Member of the American Society of Mechanical Engineers, the Society of Automotive Engineers, and the Korean Society of Automotive Engineers.

Mintae Kim received the B.S. degree in Soonchunhyang University, Asan, Korea, and M.S. in Hanyang University, Seoul, Korea, in 2006 and 2008, respectively. Since 2010, he is currently working for Hankook Tire RD Center. His research interests are intelligent tire development and Tire Sensing Technology.

Hojong Lee received his B.S. and M.S. degrees in Mechanical Engineering from Hanyang University, Seoul, Korea, in 1998 and 2000, respectively. He is currently pursuing a Ph.D. degree in Mechanical Engineering at Virginia Polytechnic Institute and State University. From 2000 to 2013, he was a Research Engineer with RD Center, Hankook Tire Co. Ltd., Korea. His research interests include the characterization of tire performance based on the fusion of physical tire modeling and intelligent tire technology.